

Laboratory studies on the uptake of aromatic hydrocarbons by ice crystals during vapor depositional crystal growth

Elke Fries^{a,*}, Elena Starokozhev^a, Werner Haunold^a, Wolfgang Jaeschke^a,
Subir K. Mitra^b, Stephan Borrmann^{b,c}, Martin U. Schmidt^d

^aInstitut für Atmosphäre und Umwelt, J.W. Goethe-Universität, Frankfurt am Main, Frankfurt, Germany

^bInstitut für Physik der Atmosphäre, Johannes Gutenberg Universität, Mainz, Germany

^cMax Planck Institut für Chemie, Mainz, Germany

^dInstitut für Anorganische und Analytische Chemie, J.W. Goethe-Universität Frankfurt am Main, Frankfurt, Germany

Received 20 March 2006; received in revised form 5 April 2007; accepted 11 April 2007

Abstract

Uptake of aromatic hydrocarbons (AH) by ice crystals during vapor deposit growth was investigated in a walk-in cold chamber at temperatures of 242, 251, and 260 K, respectively. Ice crystals were grown from ambient air in the presence of gaseous AH namely: benzene (C₆H₆), toluene (methylbenzene, C₇H₈), the C₈H₁₀ isomers ethylbenzene, *o*-, *m*-, *p*-xylene (dimethylbenzenes), the C₉H₁₂ isomers *n*-propylbenzene, 4-ethyltoluene, 1,3,5-trimethylbenzene (1,3,5-TMB), 1,2,4-trimethylbenzene (1,2,4-TMB), 1,2,3-trimethylbenzene (1,2,3-TMB), and the C₁₀H₁₄ compound *tert*-butylbenzene. Gas-phase concentrations calculated at 295 K were 10.3–20.8 μg m⁻³. Uptake of AH was detected by analyzing vapor deposited ice with a very sensitive method composed of solid-phase micro-extraction (SPME), followed by gas chromatography/mass spectrometry (GC/MS).

Ice crystal size was lower than 1 cm. At water vapor extents of 5.8, 6.0 and 8.1 g m⁻³, ice crystal shape changed with decreasing temperatures from a column at a temperature of 260 K, to a plate at 251 K, and to a dendrite at 242 K. Experimentally observed ice growth rates were between 3.3 and 13.3 × 10⁻³ g s⁻¹ m⁻² and decreased at lower temperatures and lower value of water vapor concentration. Predicted growth rates were mostly slightly higher.

Benzene, toluene, ethylbenzene, and xylenes (BTEX) were not detected in ice above their detection limits (DLs) of 25 pg g_{ice}⁻¹ (toluene, ethylbenzene, xylenes) and 125 pg g_{ice}⁻¹ (benzene) over the entire temperature range. Median concentrations of *n*-propylbenzene, 4-ethyltoluene, 1,3,5-TMB, *tert*-butylbenzene, 1,2,4-TMB, and 1,2,3-TMB were between 4 and 176 pg g_{ice}⁻¹ at gas concentrations of 10.3–10.7 μg m⁻³ calculated at 295 K. Uptake coefficients (*K*) defined as the product of concentration of AH in ice and density of ice related to the product of their concentration in the gas phase and ice mass varied between 0.40 and 10.23. *K* increased with decreasing temperatures. Values of Gibbs energy (ΔG) were between -4.5 and 2.4 kJ mol⁻¹ and decreased as temperatures were lowered. From the uptake experiments, the uptake enthalpy (ΔH) could be determined between -70.6 and -33.9 kJ mol⁻¹. The uptake entropy (ΔS) was between -281.3 and -126.8 J mol⁻¹ K⁻¹. Values of ΔH and ΔS were rather similar for 4-ethyltoluene, 1,3,5-TMB and *tert*-butylbenzene, whereas 1,2,3-TMB showed much higher values.

© 2007 Elsevier Ltd. All rights reserved.

Keywords: Aromatic hydrocarbons; Ice-phase precipitation; Crystal growth; Uptake

*Corresponding author. Present address: Institut für Umweltsystemforschung, Universität Osnabrück, Barbarastr. 12, 49076 Osnabrück, Germany. Tel.: +49 541 969 3441; fax: +49 541 969 2599.

E-mail address: fries@usf.uos.de (E. Fries).

1. Introduction

Aromatic hydrocarbons (AH) constitute a main part of atmospheric pollution. Those compounds are emitted from car traffic, jet fuel combustion, fuel handling, and solvent use and production (Brocco et al., 1997; Spicer et al., 1994; Slemr et al., 2001). One important process affecting the fate of chemicals in the atmosphere is their removal by precipitation. AH like ethylbenzene, xylenes and 1,2,4-trimethylbenzene (1,2,4-TMB) have been detected in precipitation with significantly lower average concentrations in rain ($15\text{--}53\text{ ng l}^{-1}$) than in snow ($71\text{--}2200\text{ ng l}^{-1}$) (Ligocki et al., 1985, Czuczwa et al., 1988). Kos and Ariya (2006) detected 12 AH in snow at concentrations between $0.12\text{ }\mu\text{g m}^{-3}$ (ethylbenzene) and $316\text{ }\mu\text{g m}^{-3}$ (toluene). Scavenging of organic gases by precipitation has a cleaning effect on the atmosphere. On the other hand, the atmospheric removal of chemicals poses a potential risk for contamination of aquatic and terrestrial ecosystems.

Most of the precipitation in the midlatitudes is formed via ice in the upper troposphere. Dendritic snow and ice crystals contribute significantly to wet deposition of airborne contaminants by washing out aerosol and gaseous compounds (Franz, 1994). In a snow pack, the large specific surface area of ice crystals has the potential to adsorb appreciable quantities of hydrophobic organic gases (Hoff et al., 1995). Scott (1981) proposed the removal of organic gases by wet deposition as an equilibrium process between the gas and the aqueous phase that follows Henry's law. However, the standard Henry's law coefficient (H), defined as the concentration of a compound in the gas phase to its concentration in the liquid phase, sometimes underestimates the amount of organic trace gases measured in precipitation and particularly in snow (Schomburg et al., 1991; Sagebiel and Seiber, 1993).

The uptake of inorganic compounds like HCl, HNO₃, and SO₂ by planar ice surfaces, ice spheres, and dendritic ice crystals during crystal growth have been already reported (Mitra et al., 1990; Diehl et al., 1995; Conklin et al. 1993; Dominé and Thibert, 1996; Santachiara et al., 1998). Huffman and Snider (2004) determined a significant volume uptake on ice as the dominant uptake mechanisms for some C₁–C₄-alcohols and acetone. However, data on the uptake of organic compounds during crystal growth are rather limited.

In this paper, laboratory experiments are presented to investigate the uptake of AH by ice crystals

during vapor depositional growth. Inside a walk-in cold chamber, ice crystals were grown from an ambient airflow in the presence of gaseous AH. With this approach, falling ice crystals were simulated during crystal growth. Experimentally defined ice growth rates are compared to predicted ones. Selected compounds for the uptake experiments at different temperatures were benzene, and alkylated benzenes, namely: benzene (C₆H₆), toluene (methylbenzene, C₇H₈), the C₈H₁₀ isomers ethylbenzene, *o*-, *m*-, *p*-xylene (dimethylbenzenes), the C₉H₁₂ isomers *n*-propylbenzene, 4-ethyltoluene, 1,3,5-trimethylbenzene (1,3,5-TMB), 1,2,4-TMB, 1,2,3-trimethylbenzene (1,2,3-TMB), and the C₁₀H₁₄ compound *tert*-butylbenzene. Concentrations of AH were measured in ice samples by solid-phase microextraction (SPME), followed by gas chromatography/mass spectrometry (GC/MS) and uptake coefficients were determined.

2. Experimental methods

2.1. Experimental setup

Three uptake experiments were performed in a 2 m × 2 m walk-in cold chamber (WCC) at atmospheric pressure. The core of the experimental setup was a crystal growth chamber (CGC). Two different types of CGC were designed (CGC1, CGC2) with a cross-section of 0.005 m². In Fig. 1, the setup for experiments with CGC1 is shown. Inside the CGC1, ice crystals were grown by vapor deposition on an aluminum extruded heat sink (0.5 SA DIN1748, Fischer, Germany) with 0.05 m in height, 0.40 m in length, and 0.25 m in width, which also served as a heat exchanger. Ice crystals were grown by vapor deposition from a supersaturated ambient air stream at the corresponding temperatures. The air was pumped with a flow rate of $0.0005\text{ m}^3\text{ s}^{-1}$ in a Teflon tube. By means of a cleaning device equipped with two activated carbon filters and one Teflon filter, AH and aerosol particles were removed from ambient air. The determination of the removing efficiency of the cleaning device for benzene, toluene, ethylbenzene, and xylenes (BTEX) is described in detail in Fries et al. (2006) and was 84–100%. In one separate experiment, the total particle concentration of the carrier gas was measured by a condensation particle counter (CPC, model TSI 3022). After passing the cleaning device, all particles were removed from the carrier gas. Gaseous N₂, O₂, CO₂, and H₂O were still

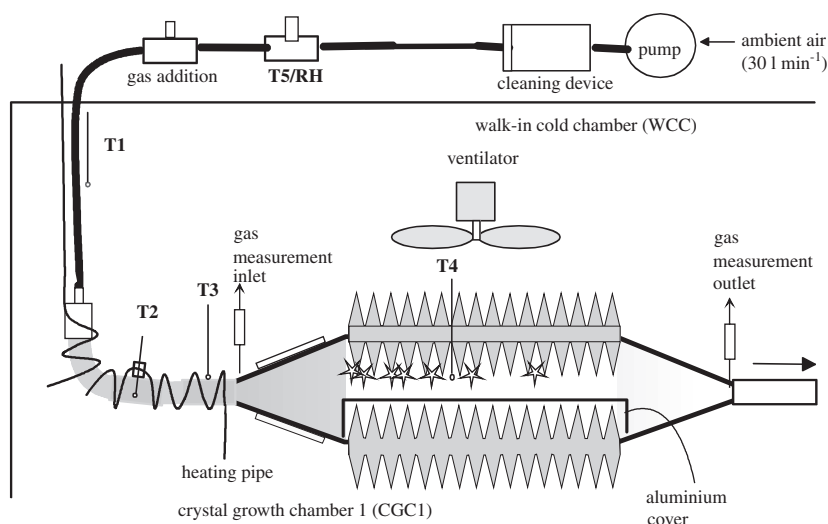


Fig. 1. Setup of uptake experiments with crystal growth chamber 1 (CGC1) showing positions of temperature sensors (T_1 – T_5) and humidity sensor (RH).

present in air. During the exposure experiments, the CPC was removed to avoid contamination of the system with butanol vapor. A gaseous standard mixture of selected AH was prepared in a gas cylinder by dissolving liquid substances in pre-cleaned synthetic air. Resulting concentrations were as follows: 6266 ppb benzene, 5221 ppb toluene, 4542 ppb ethylbenzene, 9084 ppb *m/p*-xylene, 4558 ppb *o*-xylene, 3989 ppb *n*-propylbenzene, 3984 ppb 4-ethyltoluene, 3998 ppb 1,3,5-TMB, 3630 ppb *tert.*-butylbenzene, 4114 ppb 1,2,4-TMB, and 4137 ppb 1,2,3-TMB. The mixture of AH was added to the ambient airflow with a flow rate of 15.0 ml min^{-1} adjusted by a mass flow controller. Gas addition was performed through a heated Teflon pipe to avoid condensation. Resulting concentrations of AH in the airflow outside the WCC calculated at 295 K were of 10.3 – $20.8 \mu\text{g m}^{-3}$. Partial pressures of gases (P_{gas}) were calculated by

$$P_{\text{gas}} = \frac{c}{M} RT, \quad (1)$$

where c is the concentration of AH in the gas phase (in ng m^{-3}), M is the molar mass of AH (in ng mol^{-1}), R is the gas constant ($8.3144 \text{ J mol}^{-1} \text{ K}^{-1}$), and T is the temperature measured at T_5 . The air/gas mixture entered the CGC1 through a heated aluminium interface of 5 cm in diameter. With a Reynolds number around 900, the gas flow inside the reactor was assumed to be laminar. The flow rate inside the CGC simulating the fall velocity of the ice crystals was 0.1 m s^{-1} . Each uptake experiment was performed for 22 h. Five temperature sensors (T_1 – T_5) were

installed at different positions. Humidity of ambient air was measured by a humidity sensor (RH). Sensor positions at CGC1 are shown in Fig. 1. Outside the WCC, actual temperature and relative humidity of ambient air were measured by sensors T_5 and RH, respectively. Inside the WCC, the air–gas mixture entered the CGC1 through a heated Teflon tube kept permanently at 288 K to avoid ice condensation. Temperature was controlled by sensors T_1 – T_3 . Inside the CGC1, the temperature of the crystal-growing environment was measured by sensor T_4 . Temperature and humidity during uptake experiments are listed in Table 1. Relative humidity (RH) of ambient air was at 34%, 30%, and 35% with temperatures at T_5 being 295, 298, and 295 K, respectively. Values of water pressures (P_{water}) in the air–gas stream were of 9.0, 9.5, and 9.3 hPa. The temperature of the WCC (T_{WCC}) was maintained at 253, 247, and 238 K causing temperatures of 260, 251, and 242 K measured at sensor T_4 . Temperatures at T_4 were all below frost point temperatures at corresponding water vapor pressures causing continuous ice crystallization at the heat sink. Supersaturation (ΔP_{water}) was calculated by

$$\Delta P_{\text{water}} = P_{\text{water}} - P_{\text{water,sat}}, \quad (2)$$

where $P_{\text{water,sat}}$ is the saturation vapor pressure at temperatures measured at T_4 . Values of ΔP_{water} are also shown in Table 1 and were 7.0, 8.7, and 9.0 hPa.

For determination of ice crystal growth rates, an additional experiment was performed with more precise temperature control. T_{WCC} was set at 253 K.

Table 1
Growth conditions during uptake experiments

No.	RH (%)	T_5 (K)	P_{water} (hPa)	T_{WCC} (K)	T_4 (K)	$P_{\text{water,sat}}$ at T_4 (hPa)	ΔP_{water} (hPa)	ΔP_{water} (g m^{-3})	n
1	34	295	9.0	253	260	2.0	7.0	5.8	5
2	30	298	9.5	249	251	0.8	8.7	6.0	4
3	35	295	9.3	238	242	0.3	9.0	8.1	6

No., number of experiment; RH, relative humidity; T , temperature sensor; P_{water} , water vapor pressure; $P_{\text{water, sat}}$ = saturation vapor pressure; $\Delta P_{\text{water}} = P_{\text{water}} - P_{\text{water, sat}}$; T_{WCC} , temperature of the walk-in cold chamber; n = number of ice samples.

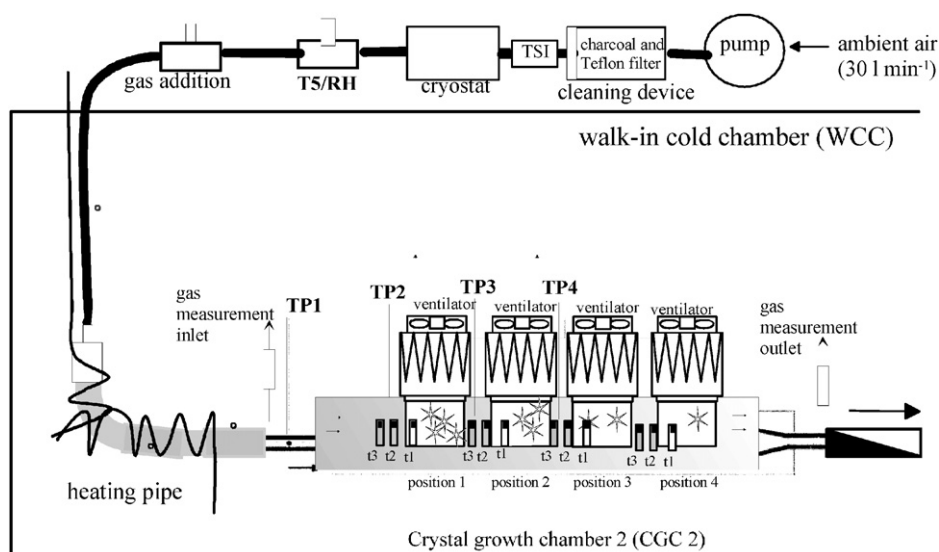


Fig. 2. Setup of the growing experiment with crystal growth chamber 2 (CGC2) showing positions of temperature (T_5 , TP1–TP4, t1–t3) and humidity sensor (RH).

The Teflon tube was placed above a vessel filled with 10 l of water to humidify the airflow. A second crystal growth chamber (CGC2) was used as shown in Fig. 2. Again, the flow rate and experimental time was 0.1 m s^{-1} and 22 h, respectively. Ice crystals were grown for 9 h on four separate aluminum extruded heat sinks (positions 1–4) with 0.1 m in diameter and a surface of 0.03 m^2 . The distance between each heat sink was appropriate to their diameter. Each heat sink was equipped with three temperature sensors t1–t3 and a ventilator to enhance heat exchange (see Fig. 2). Sensors t3 and t2 were spaced at a distance of 10 and 2 mm, respectively, and t1 was put directly inside each heat sink.

2.2. Gas analysis

During uptake experiments, concentrations of AH were controlled in the gas phase at the inlet and the

outlet of CGC1 and CGC2 (see Fig. 1 and 2). The gas/air mixture was pumped at approximately 10 l min^{-1} through glass sampling tubes packed with activated charcoal (Dräger) for 30 min. One sampling tube consisted of two layers, one sampling layer and one following layer. During sampling, AH were adsorbed by the sampling layer. The following layer verified whether the adsorption capacity of the sampling layer exceeded the breakthrough volume. After approximately 1 h, sampling tubes were removed. In the laboratory, analytes were desorbed from the sampling layer by adding $750 \mu\text{l}$ of carbon disulfide (CS_2) (Sigma-Aldrich, 99.9%). A total of $25 \mu\text{l}$ of a stock solution of 1-chlorooctane (200 mg l^{-1} in methanol) was added as an internal standard (IS). Samples were extracted in an ultrasonic bath for 10 min. One-micro-liter aliquot of each CS_2 extract was manually injected into the GC-injector using a split mode of 1:10. The injector temperature was kept at 533 K. The GC (Thermoquest

CE Instruments Trace GC2000Series) was supplied with a 60 m DB-624 capillary column (Agilent Technologies) with an ID of 0.32 mm and a film thickness of 1.8 μm . Helium served as carrier gas. The column flow was set at 1 ml min^{-1} . The GC oven temperature program was as follows: 323 K for 2 min, then heating at 283 K min^{-1} to 463 K, and finally 20 min at 463 K. Data acquisition, processing and instrument control was performed using Excalibur software (Thermoquest). Detection of the analytes was performed by a Thermoquest Finnigan Voyager MS in the electron impact positive ion and full scan mode (scan range 50–600). Quantification was done by external standard calibration. Therefore, five sampling tubes with activated charcoal were spiked with 50, 25, 10, 5, and 1 μl of a standard mixture of AH at a concentration of 100 mg l^{-1} .

2.3. Ice analysis

Ice crystals were removed after 22 h and filled into glass vials sealed up with aluminum-coated septa (Supelco). From three uptake experiments 15 ice samples were obtained with mass between 2.9 and 4.5 g. Ice samples were transported in a freezing box at 243 K to the laboratory and melted in the sealed vial right before analysis. The analytical method is described in detail by Fries and Püttmann (2006). 5 μl of 1-brom-2-chlorethane (200 mg l^{-1} in water) was added to each sample as an internal standard. Subsequently, concentrations of AH in melted ice samples were determined by solid-phase micro-extraction (SPME), followed by gas chromatography/mass spectrometry (GC/MS). The detection limits (DLs) of the analytical method were of 1–125 $\text{pg g}_{\text{ice}}^{-1}$. Mean blank values were $500 \pm 153 \text{ pg g}_{\text{ice}}^{-1}$ for benzene, $300 \pm 189 \text{ pg g}_{\text{ice}}^{-1}$ for toluene, $500 \pm 187 \text{ pg g}_{\text{ice}}^{-1}$ for ethylbenzene, $100 \pm 27 \text{ pg g}_{\text{ice}}^{-1}$ for *m/p*-xylene, $100 \pm 12 \text{ pg g}_{\text{ice}}^{-1}$ for *o*-xylene, $200 \pm 8 \text{ pg g}_{\text{ice}}^{-1}$ for *n*-propylbenzene, $40 \pm 7 \text{ pg g}_{\text{ice}}^{-1}$ for 4-ethyltoluene, $20 \pm 6 \text{ pg g}_{\text{ice}}^{-1}$ for 1,3,5-TMB, $40 \pm 7 \text{ pg g}_{\text{ice}}^{-1}$ for 1,2,4-TMB, and $20 \pm 6 \text{ pg g}_{\text{ice}}^{-1}$ for 1,2,3-TMB.

A dimensionless uptake coefficients K was calculated by

$$K = \frac{\rho_{\text{ice}} C_{\text{ice}}}{m_{\text{ice}} C_{\text{gas}}}, \quad (3)$$

where C_{ice} is the absolute mass of AH in ice (ng), ρ_{ice} is the density of ice (0.916 g cm^{-3}), C_{gas} is the concentration of AH in the gas phase (ng m^{-3}) and m_{ice} is the ice mass (g). In this context, K is a

partitioning coefficient between the gas and the ice phase. To our knowledge, data on uptake processes during ice crystal growths are rather limited due to high complexity of the uptake process. Besides adsorption, incorporation into the crystal lattice and/or solution in the quasi-liquid layer can occur.

3. Results and discussion

3.1. Ice crystal shape

Ice crystal shape and size is dependent on temperature and humidity in the crystal growth environment, as reported by Magono and Lee (1966). Ice crystal size was lower than 1 cm. Ice crystal shape changed with decreasing temperatures from a column at a temperature of 260 K (ΔP_{water} of 5.8 g m^{-3}), to a plate at 251 K (ΔP_{water} of 6.0 g m^{-3}), and to a dendrite at 242 K (ΔP_{water} of 8.1 g m^{-3}). In laboratory studies of Kobayashi (1961), ice crystal shape changed also with decreasing temperatures from a needle to a long solid column, to a sector plate, to a dendrite, to a sector plate, and back to a solid column at ΔP_{water} of 0.28 g m^{-3} . The changes occurred at temperatures near 267, 264, 261, 256, and 251 K. Values of ΔP_{water} up to 10 times higher as reported by Kobayashi (1961) could be the reason for the occurrence of columns instead of sector plates at 260 K, and dendrites instead of solid columns at 242 K in our experiments. At higher supersaturations lower temperatures are required for formation of equivalent shapes. At 251 K our observations corroborate the earlier results.

3.2. Ice growth rates

Ice growth rates were determined experimentally at T_{WCC} and results are shown in Fig. 3. After nine hours, temperature conditions in the crystal growth environment remained constant. Temperatures measured by sensors t1, t2, and t3 (see Fig. 2 for sensor positions) were as follows: 275.0 K (t3), 266.0 K (t2), and 260.0 K (t1) (position 1), 272.5 K (t3), 266.0 K (t2), and 259.5 K (t1) (position 2), 269.0 K (t3), 263.5 K (t2), and 259.0 K (t1) (position 3), 264.0 K (t3), 263.0 K (t2), and 255.0 K (t1) (position 4). After 22 h, ice masses determined gravimetrically were as follows: 31.3 g (position 1), 20.6 g (position 2), 13.1 g (position 3), and 7.8 g (position 4). Growth rates of ice were calculated by dividing ice mass at each position by the growth time of 22 h and heatsink surface of (0.03 m^2). Ice growth rates were as follows: $13.3 \times 10^{-3} \text{ g s}^{-1} \text{ m}^{-2}$ at position 1,

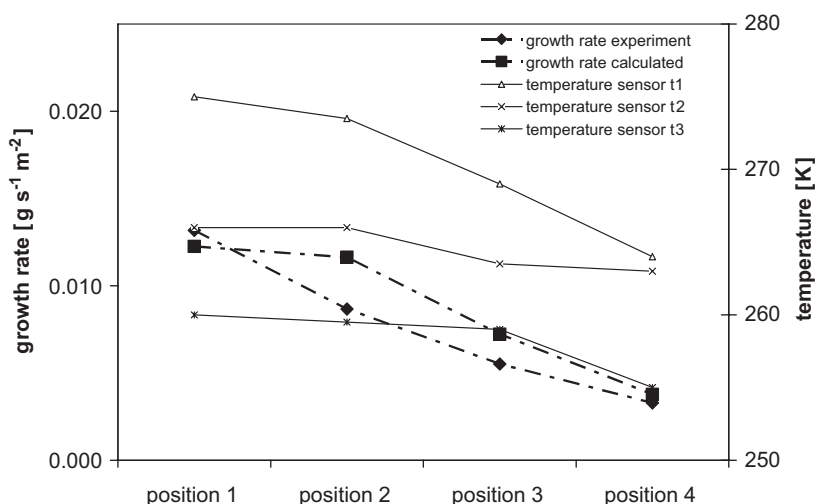


Fig. 3. Experimentally defined and predicted ice growth rates and temperatures along position 1–4 measured with sensors t1–t3.

$8.7 \times 10^{-3} \text{ g s}^{-1} \text{ m}^{-2}$ at position 2, $5.5 \times 10^{-3} \text{ g s}^{-1} \text{ m}^{-2}$ at position 3, and $3.3 \times 10^{-3} \text{ g s}^{-1} \text{ m}^{-2}$ at position 4. Ice growth rates (J) were also calculated by the Nernst equation

$$J = D_T \frac{C_0 - C_{\text{end}}}{l_m}, \quad (4)$$

where l_m is the thickness of the diffusion layer, D_T is the diffusion coefficient of water vapor ($0.00022 \text{ m}^2 \text{ s}^{-1}$). C_0 and C_{end} are calculated water vapor concentrations in the air stream at temperatures measured at sensors t3 and t1 and 100% relative humidity. C_0 and C_{end} were 5.6 and 1.7 g m^{-3} (position 1), 5.2 and 1.5 g m^{-3} (position 2), 3.5 and 1.2 g m^{-3} (position 3), and 2.3 and 1.1 g m^{-3} (position 4).

Value of l_m was calculated by the Einstein equation

$$l_m = \sqrt{2D_T t_k}, \quad (5)$$

where t_k is the condensation time. Resulting value of l_m was 0.007 m per second. Ice growth rates calculated by Eq. (4) are also shown in Fig. 3 and were as follows: $12.3 \times 10^{-3} \text{ g s}^{-1} \text{ m}^{-2}$ (position 1), $11.6 \times 10^{-3} \text{ g s}^{-1} \text{ m}^{-2}$ (position 2), $7.2 \times 10^{-3} \text{ g s}^{-1} \text{ m}^{-2}$ (position 3), and $3.8 \times 10^{-3} \text{ g s}^{-1} \text{ m}^{-2}$ (position 4).

At temperatures between 255.0 and 272.5 K , ice growth rates decreased along the crystal growth chamber with temperature and concentration of water vapor. The growth habit of ice crystals is strongly dependent on both temperature and vapor pressure. Theoretical values of growth rates were higher than experimentally defined ones, except of

growth rate at position 1. The reason for lower experimental growth rates could be loss of ice mass by wall condensation. A reason for higher theoretical growth rates could be that l_m in calculations is estimated too small. The lower predicted value of ice growth rate at position 1 could be explained by the negligence of the distance from the inlet of the flow reactor to position 1 in growth rate calculations.

3.3. Uptake of aromatic hydrocarbons

To determine background contamination during uptake experiments, ice crystals were grown from purified ambient air in five separate experiments at T_{WCC} of 253 K without organic gases. Values of AH in ice blanks were in the same range as analytical blanks. This demonstrates that no measurable AH contamination of ice occurred during crystal growth.

Fifteen ice samples grown in the presence of gaseous AH were obtained from experiments 1–3. The detection of all compounds during experiments at the inlet and the outlet of the flow reactor assured the presence of organic gases during crystal growth. Unfortunately, determination of uptake was not possible from gas-phase measurements because the sensitivity of the analytical methods was too low. Median concentrations of C_{ice} at different temperatures are shown in Table 2. After background subtraction no BTEX could be detected in ice within the DLs. A reason for this could be relatively high

Table 2

Concentrations of AH in the gas phase (C_{gas}) and partial pressures calculated at 295 K (P_{gas}) and median concentrations of AH in the ice phase (C_{ice}) at different temperatures during uptake experiments

	C_{gas} ($\mu\text{g m}^{-3}$) at 295 K	P_{gas} (hPa) at 295 K	C_{ice} ($\text{pg g}_{\text{ice}}^{-1}$) at 260 K	C_{ice} ($\text{pg g}_{\text{ice}}^{-1}$) at 251 K	C_{ice} ($\text{pg g}_{\text{ice}}^{-1}$) at 242 K
<i>n</i> -Propylbenzene	10.3	2.1×10^{-6}	14 ± 15	5 ± 22	80 ± 55
4-Ethyltoluene	10.3	2.1×10^{-6}	5 ± 6	21 ± 29	72 ± 27
1,3,5-TMB	10.4	2.1×10^{-6}	4 ± 3	11 ± 19	57 ± 18
<i>tert.</i> -Butylbenzene	10.5	1.9×10^{-6}	15 ± 15	57 ± 36	176 ± 79
1,2,4-TMB	10.7	2.2×10^{-6}	22 ± 17	20 ± 18	126 ± 14
1,2,3-TMB	10.7	2.2×10^{-6}	14 ± 34	37 ± 30	85 ± 20

Table 3

Molecular weight (MW), water solubility at 25 °C (S), and vapor pressure at 25 °C (P) of AH

	MW (g mol^{-1})	S (mg l^{-1})	P (hPa)
<i>n</i> -Propylbenzene	120	52	4.6
4-Ethyltoluene	120	95	4.0
1,3,5-TMB	120	48	3.3
<i>tert.</i> -Butylbenzene	134	30	2.9
1,2,4-TMB	120	57	2.7
1,2,3-TMB	120	72	2.3

standard deviations of blank values due to their ubiquitous occurrence in air. A second reason for the absence of those compounds in ice could be more reversible interactions caused by higher compounds volatility. Vapor pressures of BTEX are between 8.8 and 126.4 hPa. Huffman and Snider (2004) assessed a very low uptake for highly volatile compounds as toluene and cyclohexane. In Table 3, molecular weights, water solubility, and vapor pressure of the pure compounds detected in ice are shown. At gas-phase concentrations between 10.3 and $10.7 \mu\text{g m}^{-3}$ calculated at 295 K, median concentrations of *n*-propylbenzene, 4-ethyltoluene, 1,3,5-TMB, *tert.*-butylbenzene, 1,2,4-TMB, and 1,2,3-TMB varied between $4 \text{ pg g}_{\text{ice}}^{-1}$ and $176 \text{ pg g}_{\text{ice}}^{-1}$. Values of K obtained at different temperatures are shown in Table 4. Values of $K > 0$ demonstrate uptake of AH by ice from the gas phase. Values of K were between 0.4 and 10.2 and increased with decreasing temperatures indicating a greater uptake as temperatures are lowered. Vapor pressure of all compounds detected in ice was below 4.6 hPa and water solubility was below 95 mg l^{-1} . However, a trend of K with physical parameters of the individual compounds could not be observed. For non-growing ice crystals, the uptake of all those AH was below the DLs (Fries et al., 2006). Results of

the present study are an indication that AH uptake during ice crystal growth is large relative to the uptake of AH for non-growing ice crystals. This observation implies that surface adsorption of the AH studied here is negligible relative to bulk uptake during ice growths. However, our experiments do not show whether AH are incorporated into the crystal lattice or included as small liquid droplets inside or between the crystals. AH uptake by freezing of supercooled water droplets which is called “riming” could be excluded since rimed ice crystals were never observed under the present experimental conditions.

In Fig. 4, median values of $\ln K$ for *n*-propylbenzene, 4-ethyltoluene, 1,3,5-TMB, *tert.*-butylbenzene, 1,2,4-TMB, and 1,2,3-TMB are plotted versus the reciprocal values of temperatures. Values of P_{water} during these experiments were rather similar at 9.0, 9.5, and 9.3 hPa. The values of $\ln K$ showed a positive dependence on the reciprocal of temperature for 4-ethyltoluene, 1,3,5-TMB, *tert.*-butylbenzene, 1,2,4-TMB, and 1,2,3-TMB. Our results show an inverse relationship of the uptake of organic compounds by growing ice crystals from the gas phase to the temperature of the growing environment. Ligocki et al. (1985) reported Henry's Law coefficient H (in $\text{atm m}^3 \text{ mol}^{-1}$), defined as the ratio of the compound's vapor pressure to its solubility decreases by a factor of approximately two for every decrease in temperature of 283 K. Unfortunately, to our best knowledge, there is no data in the literature concerning H as a function of temperature below 273 K for the AH compounds used in this study. One explanation for a greater uptake at lower temperatures could be different ice formations at different temperatures. Grain boundaries, veins, nodes, and defects in the ice lattice may determine the uptake of AH by growing ice crystals. Franz (1994) and Hoff et al. (1995) referred a larger

Table 4
Median values of K and resulting values of ΔG received from uptake experiments at different temperatures

	K at 260 K	K at 251 K	K at 242 K	ΔG (kJ mol ⁻¹) at 260 K	ΔG (kJ mol ⁻¹) at 251 K	ΔG (kJ mol ⁻¹) at 242 K
<i>n</i> -Propylbenzene	1.13	0.39	5.11	-0.3	1.9	-3.2
4-Ethyltoluene	0.40	1.62	4.60	1.9	-1.0	-3.0
1,3,5-TMB	0.32	0.85	3.64	2.4	0.3	-2.5
<i>tert.</i> -Butylbenzene	1.10	4.00	10.23	-0.2	-2.8	-4.5
1,2,4-TMB	1.61	1.40	7.32	-1.0	-0.7	-3.9
1,2,3-TMB	1.54	2.60	4.94	-0.9	-1.9	-3.1

scavenging of organic gases by ice and snow to a higher specific surface area of dendrites. The negative dependence of the uptake on temperature is similar to results for the uptake of C₁–C₄ alcohols obtained from Henry's Law models (Crutzen and Gidel, 1983), and co-condensation models (Sigg and Neftel, 1988). Jayne et al. (1991) observed a negative dependence of the surface accommodation coefficient of C₁–C₄ alcohols on super cooled liquid water droplets and temperature. However, for the uptake of C₁–C₄-alkanols and acetone, a positive correlation to the ambient temperature has been observed (Huffman and Snider, 2004). The authors suggested that hydrogen-bonding ability of alkanols facilitates the uptake of more polar compounds by ice. Compounds in the present study cannot form hydrogen bonds and correspondingly their water solubility is relatively low.

The uptake of AH on non-growing ice crystals is strictly spoken not an equilibrium but a stationary state. Nevertheless, the crystal growth is slow and the system is not so far from the equilibrium state. Therefore, as a first approximation we will discuss K in terms of equilibrium thermodynamics. Values of Gibbs energy (ΔG) for different temperatures were calculated by

$$\Delta G = -RT \ln K. \quad (6)$$

Values of ΔG were between -4.5 and 2.4 kJ mol⁻¹. Decreasing values of ΔG with decreasing temperatures indicate again a better uptake at lower temperatures.

The theoretical temperature dependence of a sorption coefficient K is given by the Van't Hoff equation, from which it follows that

$$\ln K = -\frac{(\Delta H - T\Delta S)}{RT} = -\frac{\Delta H}{R} \frac{1}{T} + \frac{\Delta S}{R}. \quad (7)$$

A plot of $\ln K$ versus the reciprocal of temperature T should give a straight line with the slope

$-\Delta H/R$, where ΔH is the heat of sorption and R is the gas constant (8.3144 J mol⁻¹ K⁻¹) and the intercept $\Delta S/R$ where ΔS is sorption entropy. In our approach we use heat of uptake and uptake entropy. Multiplying the slopes of the regression lines in Fig. 4 with the negative value of R yields the values of ΔH . Multiplying the intercepts of the regression lines in Fig. 4 with the negative value of R yields the values of ΔS . Table 5 shows slopes $-\Delta H/R$, intercepts $\Delta S/R$, regression coefficients r^2 , and values of ΔH and ΔS . Regression lines of AH showed a good linearity with values of r^2 between 0.988 and 0.998, except for *n*-propylbenzene ($r^2 = 0.424$) and 1,2,4-TMB ($r^2 = 0.774$). For these two compounds, the linearity of regression lines is too low for a thermodynamic discussion. For 4-ethyltoluene, 1,3,5-TMB, *tert.*-butylbenzene, and 1,2,3-TMB values of ΔH , and ΔS were between -33.9 and -70.6 kJ mol⁻¹ and -126.8 and -281.3 J mol⁻¹ K respectively. Values of the uptake enthalpy ΔH and the uptake entropy ΔS increased with decreasing compound vapor pressure of the pure compounds. This is an indication that the uptake of AH is dependent on the physical parameters of the compounds. According to our results 1,2,3-TMB has a much higher value of ΔH compared to other AH isomers. This unexpected result requires further investigations, e.g. modelling the uptake procedure by atomistic models. In a previous adsorption study of AH on ice surfaces, Goss (1993) reported for the sorption itself higher values of ΔH for *m*-xylene (-38.1 kJ mol⁻¹) and *p*-xylene (-37.7 kJ mol⁻¹) than values of ΔH for 4-ethyltoluene, 1,3,5-TMB, and *tert.*-butylbenzene in this study. Lower values of ΔH obtained from our first approximation in terms of equilibrium thermodynamics are a sign that the uptake of AH during crystal growths cannot be described only by sorption.

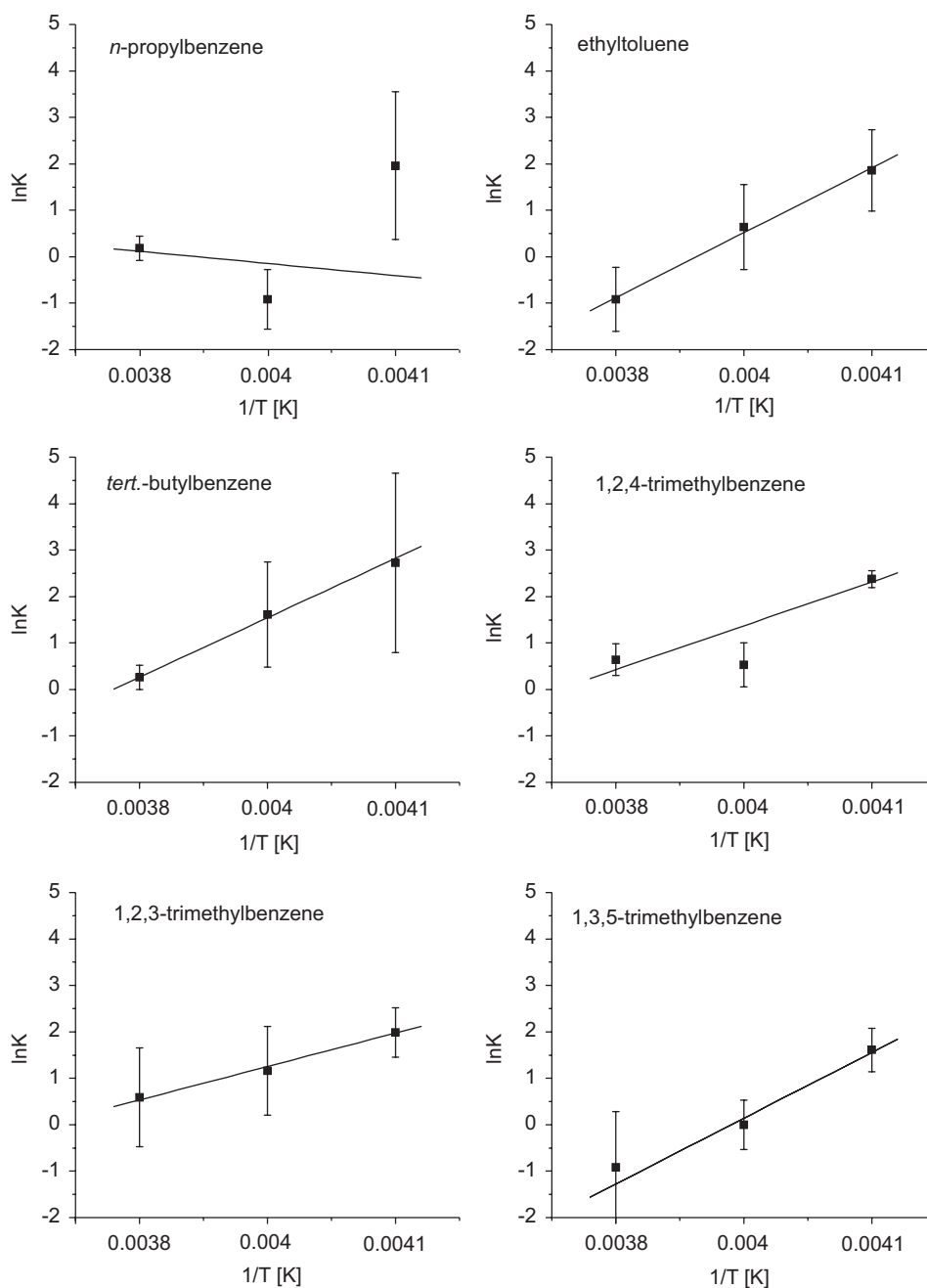


Fig. 4. Median values of $\ln K$ versus reciprocal temperature derived during uptake experiments.

Table 5

Slopes, $\Delta H/R$, intercepts, $\Delta S/R$, and regression coefficients, r^2 of regression lines, uptake enthalpy, ΔH , and uptake entropy ΔS

	$\Delta S/R$	$-\Delta H/R$ (K)	r^2	ΔH (kJ mol ⁻¹)	ΔS (J mol ⁻¹ K ⁻¹)
4-Ethyltoluene	-33.49	8490	0.990	-70.6	-278.3
1,3,5-TMB	-33.85	8488	0.991	-70.5	-281.3
tert.-Butylbenzene	-29.73	7774	0.988	-64.6	-247.1
1,2,3-TMB	-15.26	4075	0.998	-33.9	-126.8

4. Conclusions

The uptake of aromatic hydrocarbons (AH) by ice crystals was studied during vapor depositional growth at temperatures below 260 K. Ice crystals were grown from an airflow. With this approach mass flow of water vapor was enhanced. Ice crystal shape and size was a function of temperature in the crystal growth environment. Predicted ice growth rates were overestimated depending upon the assumption for the thickness of the diffusion layer. Uptake of lower volatile AH from the gas phase was observed during ice crystal growth. From the uptake experiments at different temperatures, the enthalpy and entropy of the uptake process could be determined. Our results are an indication that in-cloud scavenging is a possible uptake process for organic compounds by ice crystals. Since most precipitation is formed via ice in the troposphere at low temperatures in-cloud scavenging could be a possible explanation for the occurrence of organic compounds in freshly fallen snow. Therefore, interactions of ice and organic compounds can influence atmospheric transport and removal of those compounds from the atmosphere by precipitation. A rough estimation of ice phase precipitation scavenging half-life times based on our experimental conditions with estimated photochemical half-life times based on atmospheric conditions shows that removal of AHs by photochemical processes is higher than by ice phase precipitation. Further modelling studies are needed based on global rate of ice phase precipitation for a more detailed comparison of both sink processes.

Acknowledgments

Financial support from the Deutsche Forschungsgemeinschaft (DFG) under SFB 641 is kindly acknowledged. We thank Prof. Dr. Wilhelm Püttmann for using his GC/MS laboratory. We also thank Dr. Ralf Kurtenbach for preparing the gas standard mixture, Dr. Karoline Diehl for fruitful discussions, and two anonymous reviewers for their helpful comments.

References

Brocco, D., Fratarcangeli, R., Lepore, L., Petricca, M., Ventrone, I., 1997. Determination of aromatic hydrocarbons in urban air of Rome. *Atmospheric Environment* 31, 557–566.

Conklin, M.H., Sommerfeld, R., Laird, S.K., Villinski, J.E., 1993. Sulphur dioxide reactions on ice surface: implications for dry deposition to snow. *Atmospheric Environment* 27A, 1159–1166.

Crutzen, P.J., Gidel, A.T., 1983. A two-dimensional photochemical model of the atmosphere. 2: the tropospheric budgets of the anthropogenic chlorocarbons, CO, CH₄, CH₃Cl, and the effects of various NO_x sources on tropospheric ozone. *Journal of Geophysical Research* 88, 6641–6661.

Czuczwa, J., Leuenberger, C., Giger, W., 1988. Seasonal and temporal changes of organic compounds in rain and snow. *Atmospheric Environment* 22, 907–916.

Diehl, K., Mitra, S.K., Pruppacher, H.R., 1995. A laboratory study of the uptake of HNO₃ and HCl vapor by snow crystals and ice spheres at temperatures between 0 and –40 °C. *Atmospheric Environment* 29, 975–981.

Dominé, F., Thibert, E., 1996. Mechanism of incorporation of trace gases in ice grown from the gas phase. *Geophysical Research Letters* 23, 3627–3630.

Franz, T.P., 1994. Deposition of semivolatile organic chemicals by snow. Ph.D. Thesis, University Minnesota, Minneapolis, MN.

Fries, E., Püttmann, W., 2006. Improvement of HS-SPME for the analysis of volatile organic compounds (VOC) in water samples by simultaneous direct fiber cooling and freezing of analyte solution. *Analytical and Bioanalytical Chemistry* 386, 1497–1503.

Fries, E., Haunold, W., Jaeschke, W., Hoog, I., Mitra, S.K., Borrmann, S., 2006. Uptake of gaseous aromatic hydrocarbons by non-growing ice crystals. *Atmospheric Environment* 40, 5476–5485.

Goss, K.-U., 1993. Adsorption of organic vapors on ice and quartz sand at temperatures below 0 °C. *Environmental Science & Technology* 27, 2826–2830.

Hoff, J.T., Wania, F., Mackay, D., Gillham, R., 1995. Sorption of non-polar organic vapors by ice and snow. *Environmental Science & Technology* 29, 1982–1989.

Huffman, W.A., Snider, J.R., 2004. Ice–hydrocarbon interactions in the troposphere. *Journal of Geophysical Research* 109, D01302.

Jayne, J.T., Duan, S.X., Davidovits, P., Worsnop, D.R., Zahniser, M.S., Kolb, C.E., 1991. The uptake of gas phase alcohol and organic acid molecules by water surfaces. *Journal of Physical Chemistry* 95, 6329–6336.

Kobayashi, T., 1961. The growth of snow crystals at low supersaturations. *Philosophical Magazine* 6, 1363–1370.

Kos, G., Ariya, P.A., 2006. Determination of a wide range of volatile and semivolatile organic compounds in snow by use of solid-phase micro-extraction (SPME). *Analytical and Bioanalytical Chemistry* 385, 57–66.

Ligocki, M.P., Leuenberger, C., Pankow, J.F., 1985. Trace organic compounds in rain–II: gas scavenging of neutral organic compounds. *Atmospheric Environment* 19, 1609–1617.

Magono, C., Lee, C.W., 1966. Meteorological classification of natural snow crystals. *Journal of the Faculty of Science, Hokkaido University Series 7 (2)*, 320–335.

Mitra, S.K., Barth, S., Pruppacher, H.R., 1990. A laboratory study on the scavenging of SO₂ by snow crystals. *Atmospheric Environment* 9, 2307–2312.

Sagebiel, J.C., Seiber, J.N., 1993. Studies on the occurrence and distribution of wood smoke marker compounds in foggy

- atmospheres. *Environmental Toxicology and Chemistry* 12, 812–822.
- Schomburg, J.C., Glotfelty, D.E., Seiber, J.N., 1991. Pesticide occurrence and distribution of fog collected near Monterey, California. *Environmental Science & Technology* 25, 155–160.
- Santachiara, G., Prodi, F., Udisti, R., Prodi, A., 1998. Scavenging of SO₂ and NH₃ during growth of ice. *Atmospheric Research* 47–48, 209–217.
- Scott, B.C., 1981. Modelling wet deposition. In: Eisenreich, S.J. (Ed.), *Atmospheric Pollutants in Natural Waters*. Ann Arbor Science, Ann Arbor, MI, pp. 3–21.
- Sigg, A., Neftel, A., 1988. Seasonal variations in hydrogen peroxide in polar ice cores. *Annals of Glaciology* 10, 157–162.
- Slemr, F., Giehl, H., Habram, M., Slemr, J., Schlager, H., Schulte, P., Haschberger, P., Lindermeir, E., Doppelheuer, A., Plohr, M., 2001. In-flight measurement of aircraft CO and nonmethane hydrocarbon emission indices. *Journal of Geophysical Research* 106 (D7), 7485–7494.
- Spicer, C.W., Holdren, M.W., Riggan, R.M., Lyon, T.F., 1994. Chemical composition and photochemical reactivity of exhaust from aircraft turbine engines. *Annales Geophysicae* 12, 944–955.